

---

**ABSTRACT**

The atrazine removal from aqueous solution on three adsorbents denoted PAC (powder activated carbon), AC-HNO<sub>3</sub> (activated carbon modified with HNO<sub>3</sub>) and AC-Ag (activated carbon modified with silver) was done. The experimental results obtained showed that, the atrazine removal better fitted the Freundlich model for PAC and the Langmuir model for AC-HNO<sub>3</sub> and both Langmuir and Freundlich models for AC-Ag. Additionally, we saw that, the physicochemical properties of AC-Ag influenced the removal performances of atrazine. The maximum adsorption capacities were, 476,19 mg/g, 434,78mg/g and 357,14mg/g for PAC, AC-HNO<sub>3</sub> and AC-Ag respectively. The Kinetic study performed using the pseudo-first-order, pseudo –second- order and the intraparticle diffusion models. The regression results showed that the pseudo-second-order model fitted better the experimental data for all the three adsorbents. This study revealed that the adsorption of atrazine was influenced by the surface functionalities and was also controlled by a film diffusion mechanism.

**KEYWORDS:** Adsorption, Atrazine, surface modification, Activated carbon, kinetics, isotherms.

---

**INTRODUCTION**

The pollution of water environment by pesticides, particularly the herbicides have been recognized in the agricultural areas of the world in the last three decades. Therefore, evidence considerations have been accumulated to suggest that many water resources are contaminated with pesticides [1]. The Atrazine (2-chloro-4 ethylamino-6- isopropyl-s-triazine) as a hydrophobic and weak basic compound was selected as the model organic contaminant, because of its widespread use in the agriculture [2]. It has extensively been used to control broad-leaved weeds and grasses in crop production [3 - 4] and has frequently been detected in water due to its long half-life, apparent mobility, moderate water solubility, great leaching potential and high chemical stability in soils and aquifers [5]. The atrazine is potentially toxic to both humans, animals and ecosystems [6] because it is a possible cause for damage to reproductive structures in fish, frogs, and other wildlife, as it increased the risk of breast cancer [2]. Recent studies suggested that atrazine interferes with endocrine hormone metabolism [5]. Consequently, its use has been banned in European Union (EU) countries since 2003 [6]. Generally, The EU directive for drinking water allows 0,1µg/L of a single herbicide and 0,5µg/L for the total amount of the herbicide as admissible dose [7]. Moreover, as atrazine is often found in drinking water, the United States Environmental Protection Agency (USEPA) has also set a maximum contaminant level of 3ppb [8].

According to the aforementioned potential dangers, there is a need of developing efficient remediation treatments to remove atrazine from water. Many techniques of removing atrazine have been used in the scientific literature [9]. Adsorption process seems to be one of an effective way of removing this recalcitrant compound. Adsorption is a process whereby a contaminant adheres to the surface of an adsorbent such as activated carbon due to hydrophobic

and electrostatic interactions between the adsorbate and the adsorbent [4]. Nevertheless, considerable research have been carried out on adsorption of herbicides on activated carbons, but as far as our knowledge, there are not much research works focused on the atrazine removal onto modified activated carbons either with HNO<sub>3</sub> or Silver. Jordi et al, 2015 showed that, the adsorption capacity of an activated carbon depends on its physico-chemical characteristics and the nature of the sorbate [10].

In this present work, we study the atrazine removal from aqueous medium by activated carbon based oil palm shell by physical activation with steam and modified using hydrothermal carbonization process. The equilibrium together with the kinetics studies of atrazine removal were thoroughly analyzed using various equilibrium and kinetic models.

## MATERIALS AND METHODS

### Adsorbent

The Oil palm shells were collected in West Cameroon from local market. The shells were cleaned and washed first with tap water followed by distilled water and placed for several days under the sun dried. After, the shells were crushed and sieved to a sizes ranging 2- 2.5 mm.

### Activated Carbon preparation

30 g of dried oil palm shells was carbonized in a tube furnace (Carbolite 1200C, UK) with a temperature control under a flow of N<sub>2</sub> gas, at 400°C for 2 hours, at a heating rate of 10°C/ min. Then, the temperature was raised at 850°C at the same heating rate of 10°C/min for a residence time of 06hrs under steam flow rate of 0.1 mL/min. After the activation was achieved, the furnace together with the activated carbon were cooled to room temperature. The activated carbon was washed with distilled water and put in an oven at 105°C for 24hrs. The dried activated carbon was now ground, and sieved to powder form with a particle size less than 50 µm.

### Acid Treatment of activated carbon

The Powder Activated Carbon(PAC) was carboxylate with AC-COOH by treating it with concentrated HNO<sub>3</sub> as described by Amin et al work [11]. 25 g of activated Carbon were suspended in 500 mL concentrated nitric acid (1mol/L). The mixture was vigorously stirring for 12hrs at low temperature(80°C) then, the impregnated activated carbon was collected on filter paper and washed with distilled water until a pH of 7 was obtained. The functionalized activated carbon was finally, dried at 105°C in the oven for 24h.

### Impregnation of Activated Carbon by Hydrothermal Carbonization

Typically, amounts of PAC functionalized were added to aqueous solution of the AgNO<sub>3</sub> at 0.075 mol/L in the reactor for Hydrothermal Carbonization. The mixture was put in a tube furnace in the dark (at Hydrothermal Carbonization), after 01hr the temperature was increased to 240°C for 2.5 hrs. After, the samples obtained were collected, washed with distilled water, dried and kept well for further tests.

### Adsorbate

The atrazine (99.9%) was purchased from Chem service, France and used directly without any purification. The water solubility of atrazine is 35mg/L at 20°C.

The synthetic effluent of atrazine (20 mg/L) was prepared by dissolving (0.02 g) of atrazine in a conical flask of 1000 mL and filled with distilled water at pH=5.5 After different required standard concentrations of atrazine were prepared by dilution.

### Characterization

The adsorbents were characterized using X-ray diffraction technique with a D5000 (Siemens1) diffractometer, using the CuK<sub>α1</sub> radiation ( $\lambda = 1.5406$ ) to know their crystallinity. The identification of crystalline phases and minerals was carried out using the database Powder Diffraction File (PDF-2) of the International Centre for Diffraction Data (ICDD). FT-IR spectroscopy was applied in order to identify the functional groups and chemical bonding on the adsorbents. For this purpose, spectra were determined between 4000 and 400cm<sup>-1</sup> using an FT-IR spectroscope (Spectrum Vertex 70 DTGS). The morphological analysis of the activated carbon was performed by Scanning Electron Microscopy (SEM) (JEOL JSM-5400, Japan).

The analysis of chemical properties was done by measuring the point of zero charge,  $pH_{PZC}$  determined using the drift method. While to quantify the total acidity and the total basicity, the Boehm titration method was carried out [12].

### Batch adsorption experiment

The batch experiments for the adsorption studies were carried out at room temperature in flask of 150 ml. For each run, 0.005 to 0.015 g of the adsorbent was introduced into the flask containing 100 mL of the atrazine solution at initial concentration of 20mg/L. When the adsorption equilibrium was reached, the PAC, AC-HNO<sub>3</sub> and AC-Ag were separated from the aqueous solution using filtration method with 0.45 $\mu$ m whatman cellulose nitrate membrane. Then, the analysis of the residual solution was performed by UV-visible absorption spectrophotometry at 225 nm (UV-visible spectrophotometer Secomam). The quantity adsorbed at equilibrium;  $Q_e$  (mg.g<sup>-1</sup>) was calculated according to the following relation.

$$Q_e = (C_0 - C_e)V/m \quad (1)$$

Where,  $C_0$  and  $C_e$  (mgL<sup>-1</sup>) are the initial and equilibrium concentrations of atrazine in solution, respectively,  $V$  (L) is the total volume of the solution, and  $m$  (g) is the mass of adsorbent.

The percentage removal of atrazine from solution was calculated by using the following equation:

$$\% \text{Removal} = (C_0 - C_t)/C_0 \times 100 \quad (2)$$

Where,  $C_0$  and  $C_t$  (mgL<sup>-1</sup>) are the initial atrazine concentration and concentration at time  $t$ , respectively.

### Equilibrium Isotherm

Isotherms experimental data were fitted to two-parameters isotherm models: Langmuir (Eq. (3)), Freundlich (Eq. (5))

$$Q_e = \frac{Q_m K_L C_e}{1 + K_L C_e} \quad (3)$$

$$\frac{1}{Q_e} = \frac{1}{Q_m K_L C_e} + \frac{1}{Q_m} \quad (4)$$

$$Q_e = K_f C_e^{1/n} \quad (5)$$

$$\ln Q_e = 1/n \ln C_e + \ln K_f \quad (6)$$

where  $Q_e$  (mg/g) is the amount of compound adsorbed per unit mass of activated carbon,  $C_e$  (mg/L) is the organic compound concentration at equilibrium,  $Q_m$  (mg/g) is the maximum adsorption capacity,  $K_L$  (L/mg) is a constant related to the affinity between the pollutant and the adsorbent,  $K_f$  ((mg/g) (L/mg)<sup>1/n</sup>) is the Freundlich sorption constant and “ $n$ ” is a constant related to adsorption intensity.

### Kinetics adsorption experiment

The adsorption kinetics experiments were performed in flasks containing 100 mL of the initial atrazine concentration of 20 mg/L and 0.01g of PAC, AC-HNO<sub>3</sub>, and AC-Ag at pH 5.5. The suspensions were shaken at 250rpm for certain intervals time (30 -240 min) at 298 K. To illustrate the adsorption process and provide insights into possible reactions mechanisms, the pseudo first-order eq(7), pseudo second-order eq(8), and intraparticle diffusion eq (9) were evaluated based on the experimental data :

$$\ln(Q_e - Q_t) = -K_1 t + \ln Q_e \quad (7)$$

$$\frac{t}{Q_t} = \frac{1}{k_2 Q_e^2} + \frac{t}{Q_e} \quad (8)$$

$$Q_t = k_i t^{1/2} + c \quad (9)$$

Where  $Q_e$  (mg/g) and  $Q_t$  (mg/g) are the concentration of atrazine adsorbed on adsorbent at equilibrium and various times  $t$ ;  $K_1$  (h<sup>-1</sup>) is the rate constant of eq. (7) for the adsorption;  $K_2$  (g mg<sup>-1</sup>h<sup>-1</sup>) is the rate constant of eq. (8) for

adsorption ;  $c$  ( $\text{mg}\cdot\text{g}^{-1}\text{h}^{1/2}$ ) is the intercept and  $k_i$  is the intraparticle diffusion rate constant which can be evaluated from the slope of the linear plot of  $Q_t$  versus  $t^{1/2}$ .

## RESULTS AND DISCUSSION

### Characterization result

#### FT-IR

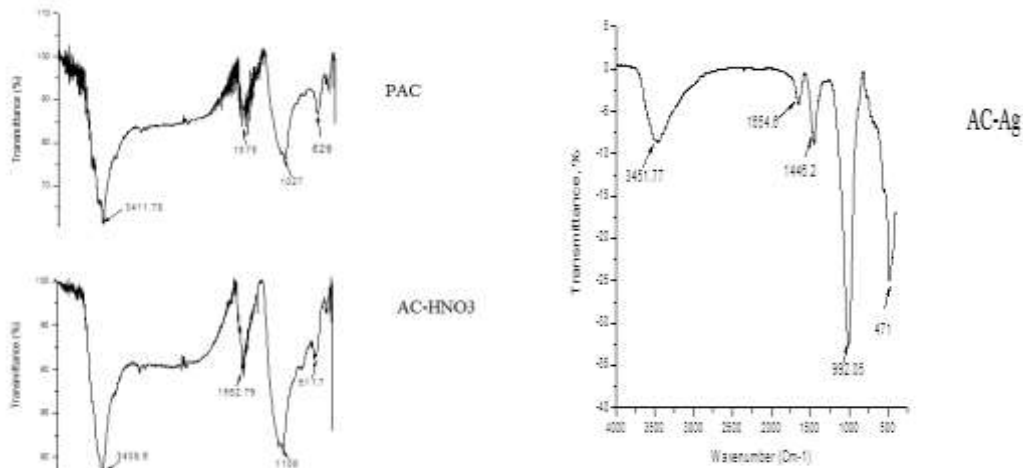


**Fig. 1: Infrared Spectroscopy of Activated Carbon samples**

For the PAC and AC-HNO<sub>3</sub>, the intensity of the characteristic peak of 3408.6 cm<sup>-1</sup> enhanced after oxidative modification which indicates the formation of large number of hydroxyl or phenolic hydroxyl groups on the surface of the oxidized AC [13]. The O–H stretching vibration (3408–3452 cm<sup>-1</sup>) and C–OH stretching vibration (999–1027 cm<sup>-1</sup>) were more obvious and broader in all samples. We also observed the two closed and acute bands at 2995 cm<sup>-1</sup> which appears in the two spectra (PAC and AC-HNO<sub>3</sub>) and correspond to the asymmetric and symmetric C-H stretching vibrations of aliphatic groups, -CH<sub>3</sub> and CH<sub>2</sub>. We remark the disappearance of this band after impregnation with Ag (AC-Ag). The three peaks located at 1654.6; 1575 and 1562.79 cm<sup>-1</sup> could be assigned to C = O vibration and in-plane C = C stretching vibration of aromatic ring, respectively for PAC, AC-HNO<sub>3</sub> and AC-Ag, which support the concept of aromatization activated carbon. The bands in the range 1000–1500 cm<sup>-1</sup>, which include the C-OH stretching and OH bending vibrations, which imply the existence of large numbers of residual hydroxy groups (OH) and carboxylate groups (COOH) [14]. The OH and COOH can react with metal ions to form metal nanoparticles [15]. It can be concluded that the surface functional groups changed largely. Moreover, the aromatic C = C stretching (skeletal ring vibration) at about 1654 cm<sup>-1</sup> increased sharply.

Acidic and basic surface functionalities were determined by Boehm titration [16] and summarized in Table 1. As expected, the total amount of acidic surface groups increased after modification with HNO<sub>3</sub> and AC-Ag respectively. The structure and chemical composition of the resultant AC-Ag synthesized in this study were confirmed by XRD and the results are shown in Fig 2.

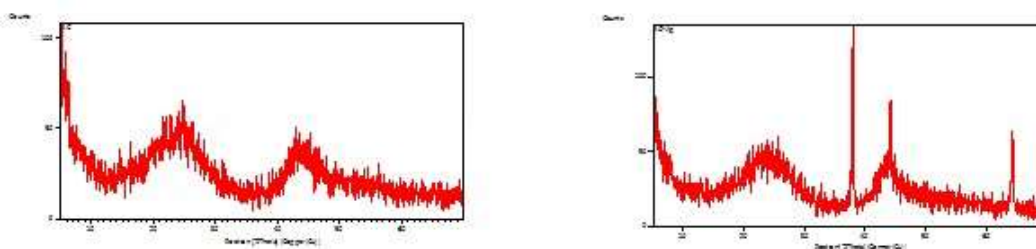


**Fig 2: XRD patterns of PAC and AC-Ag**

The XRD patterns of AC-Ag showed a face centered cubic structure presented by the diffraction peaks at 38.03°, 44.21° and 64.37° which match well with the diffraction from the (111), (200) and (220) planes, respectively [17]. Therefore, broad peaks of around 24.76° and 44.8° present the amorphous nature of PAC. The broad peaks of AC and the sharp peaks of silver appeared in the results of the AC-Ag display the coexistence of both Ag and AC.

**Table 1: Acidic and basic groups of the samples**

Samples	Carboxylics (meq/g)	Lactonic (meq/g)	Phenolic (meq/g)	Total Acids groups (meq/g)	Total Basic groups (meq/g)	pH <sub>pzc</sub>
PAC	0.5	0	0.25	0.75	1	7.9
AC-HNO3	0.75	0.25	0.25	1.25	0.5	7.1
AC-Ag	0.75	0.25	0.5	1.5	0.25	6.9

The SEM showed many orderly and developed pores due to the effect of the steam activation of oil palm shells in a first time demonstrated by homogenous circle shapes with same sizes of uniformly distributed pores (Fig 3.A) which have grown more broad after modification with HNO3 (Fig 3.B). However, after impregnation with silver, we can see that the Ag particles were covered on the surface of PAC and blocked some pores (Fig 3.C).

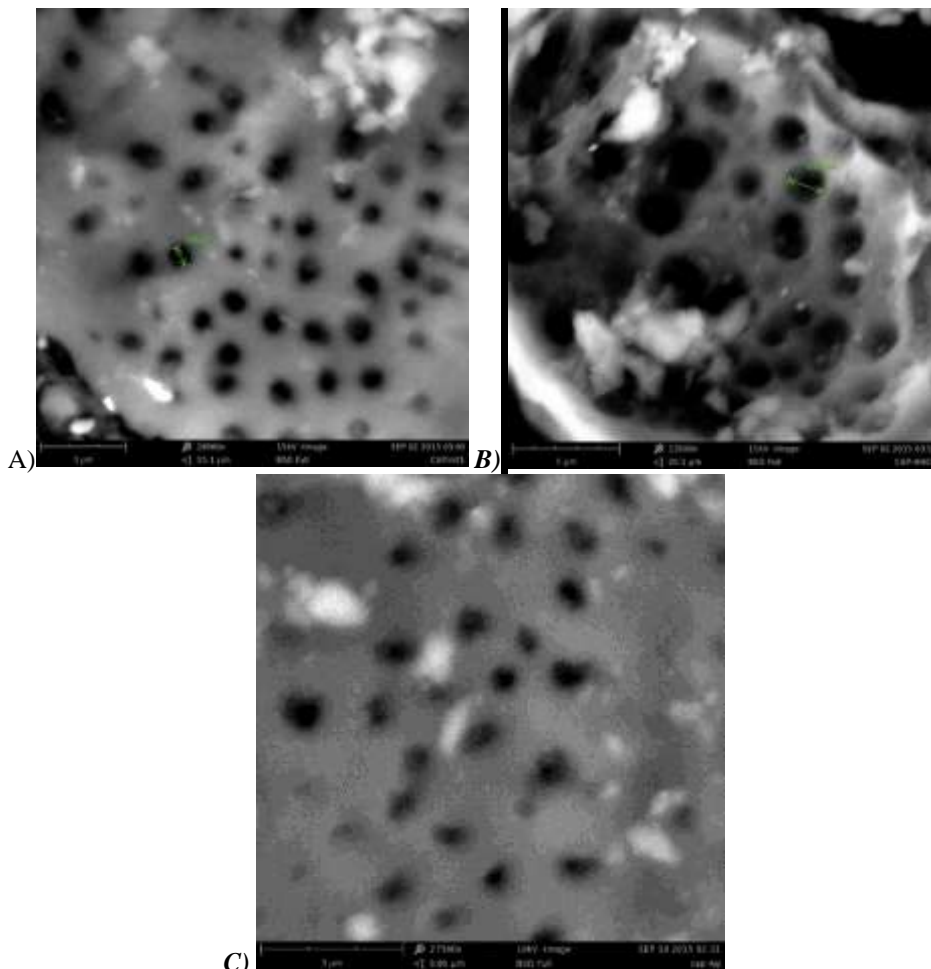


**Fig. 3: SEM of : A) PAC, B) AC-HNO3 et C) AC-Ag**

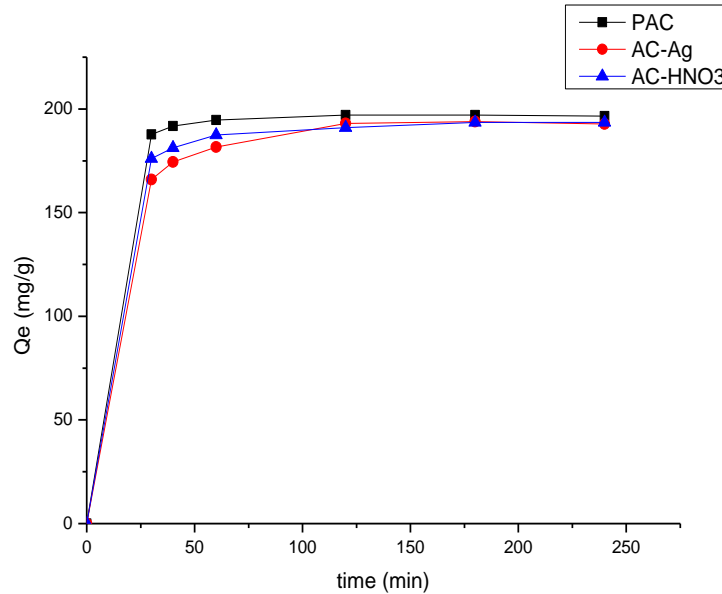
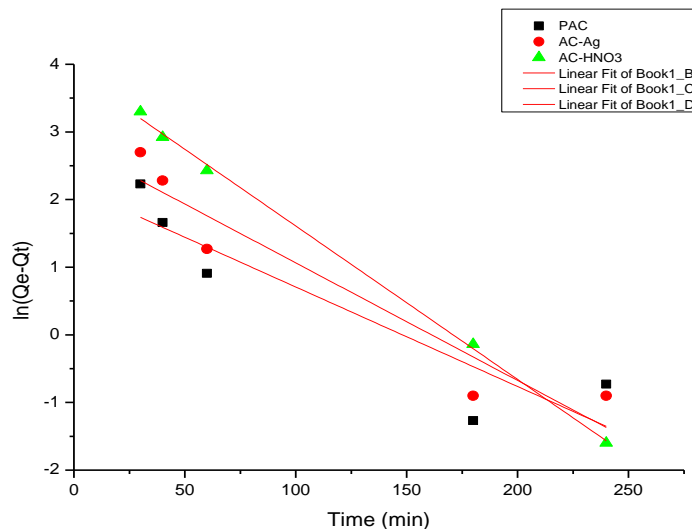
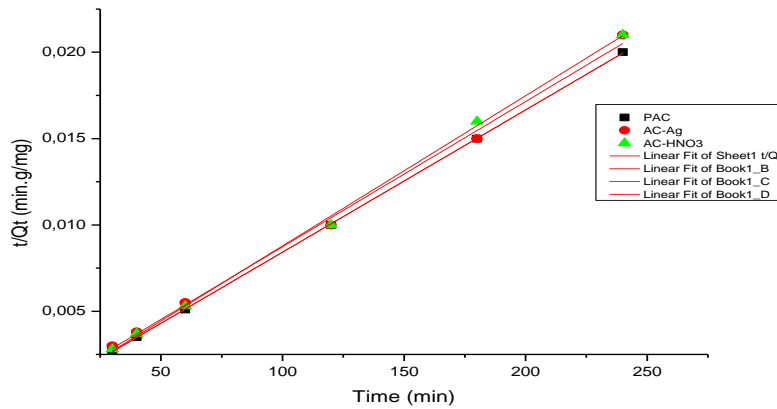


**Fig 4: Effect of contact time on the atrazine adsorbed by PAC, AC-Ag and AC-HNO<sub>3</sub>**

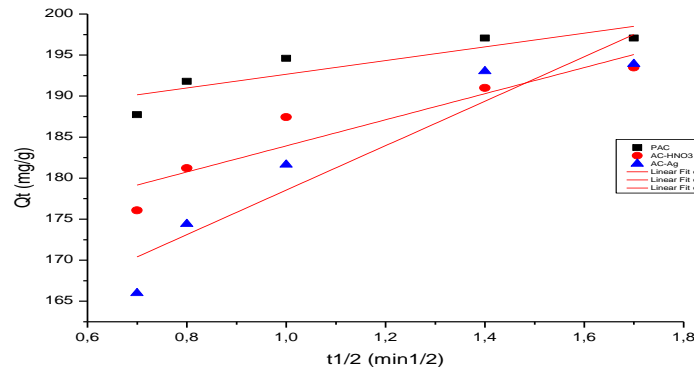
The effect of contact time on the adsorption of atrazine by PAC, AC-Ag and AC-HNO<sub>3</sub> was displayed in Fig 4. It was found that, for all the adsorbents, the adsorption process was very fast during the first 30 min followed by a slow increase before the equilibrium was reached at about 120 min. And the adsorbed amount of atrazine reached 197.08mg/g for PAC, 193.03 mg/g for AC-Ag and 191mg/g for AC-HNO<sub>3</sub> when the initial atrazine concentration was 20mg/L. The rapid uptake revealed that there was a strong adsorption affinity between atrazine and the adsorbents [5]. The adsorption increases rapidly because there are more free active sites on the adsorbents, and then progressively, there is a saturation in the adsorbents sites which consequently, decrease adsorption kinetic. Similar results were recorded by other authors [9].



(A)



B)



C)

Fig 5. Linear regression of kinetics plots: A) Pseudo-first order model; B) Pseudo-Second order model ; C) Intraparticle diffusion model

Table 2: Kinetic parameters for atrazine sorption on PAC; AC-HNO<sub>3</sub> ; AC-Ag

Kinetic models	Parameters	PAC	AC-HNO <sub>3</sub>	AC-Ag
Pseudo – first order	Q <sub>e exp</sub> (mg/g)	197.08	191.00	193.03
	K <sub>1</sub> (h <sup>-1</sup> )	0.8823	1.043	1.3609
	Q <sub>e cal</sub> (mg/g)	8.81	16.41	48.13
	R <sup>2</sup>	0.8441	0.9157	0.9985
	RSME	184.08	170.8	135.91
Pseudo-Second order model	Q <sub>e exp</sub> (mg/g)	197.08	191	193.03
	K <sub>2</sub> (h <sup>-1</sup> )	0.12	0.27	0.08
	Q <sub>e cal</sub> (mg/g)	204.08	192.3	200
	R <sup>2</sup>	0.9999	0.9986	0.9973
	RSME	10.43	8.31	19.52
Intraparticle diffusion model	K <sub>i</sub>	8.3475	15.908	27.11
	C	184.31	168.03	151.43
	R <sup>2</sup>	0.7858	0.8777	0.9009
	RSME	9,99	18,92	32,20

RSME: Root mean square error equal to  $\sqrt{\frac{1}{N} \sum (Q_{e,\text{calculated}} - Q_{e,\text{experimental}})^2}$

The linear regression of adsorption kinetics is shown in Fig 5 and Table 2. The R<sup>2</sup> values of pseudo-second order model were 0.9999, 0.9986 and 0.9973 for PAC, AC-HNO<sub>3</sub> and AC-Ag respectively, they are larger than those of pseudo first order. Nevertheless, the root mean square error of pseudo second order models was significantly smaller than those of pseudo first order model for the three adsorbents. Moreover, the experimental Q<sub>e</sub> (Q<sub>e,exp</sub>) values are close to the calculated Q<sub>e</sub> (Q<sub>e,cal</sub>) values for pseudo second order but not for pseudo first order for PAC, AC-HNO<sub>3</sub> and AC-Ag (Table2). In general, these data indicated that the adsorption kinetics of atrazine by all the three adsorbents can be better described by pseudo second order model. Thus, we can conclude that the modification of the surface of activated carbon doesn't change the kinetics of the removal of atrazine. Similar observations were noticed by Guang-cai *et al.*, in 2009, Jordi *et al.*, in 2015 [6; 10].

The intraparticle diffusion model was used to determine the rate limiting step of the adsorption process [2]. An analysis of the results from this model demonstrated a linear regression, but the plot did not pass through the origin (Fig 5.C) thereby suggesting that the intraparticle diffusion was related to the adsorption but not a sole rate-controlling step [18-19]. In addition, the high values of the intraparticle rate constant (k<sub>i</sub>= 8.347 ;15.908; 27.11mg./g.h respectively for PAC, AC-HNO<sub>3</sub> and AC-Ag which indicated the intraparticle diffusion mechanism predominates in the atrazine adsorption. In addition, the modification of surface of adsorbent enhanced the intraparticle diffusion due to the presence of oxygen on the surface of the adsorbents.

#### Effect of mass

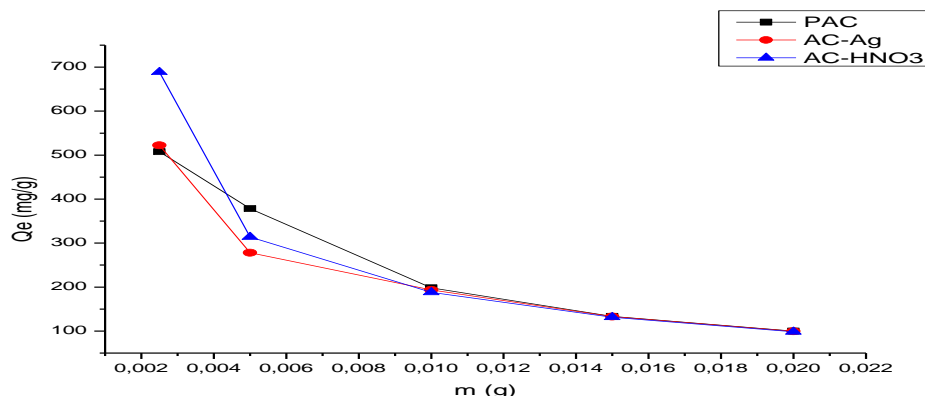


Fig 4: Effect of adsorbent dose (C<sub>0</sub>=20mg/L; pH =5,5; t= 120min)

The effect of carbon dose was studied using a dose of the PAC, AC-HNO<sub>3</sub> and AC-Ag from 0.0025 to 0.025 g was represented in Fig 4. These results shown that the percentage of atrazine removal was increased by increasing the dose of adsorbents until 0.015g. It appeared that by increasing these adsorbents dose, the number of adsorption sites available for sorbent-solute interaction increased, thereby resulting in the increased percentage of atrazine removal from the solution [20]. But the adsorption capacity (Q<sub>e</sub>) decreased with the amounts of PAC, AC-HNO<sub>3</sub> and AC-Ag. This may be due to the agglomeration of the adsorbent particles from high sorbent dose. This agglomeration would lead to a decrease in total surface area of the sorbent and increase in diffusional path length [21].

#### Adsorption isotherms

The corresponding values of Freundlich and Langmuir isotherms were listed in Table 3, and the Figure 5 shown the linear plot of Langmuir and Freundlich adsorption models.



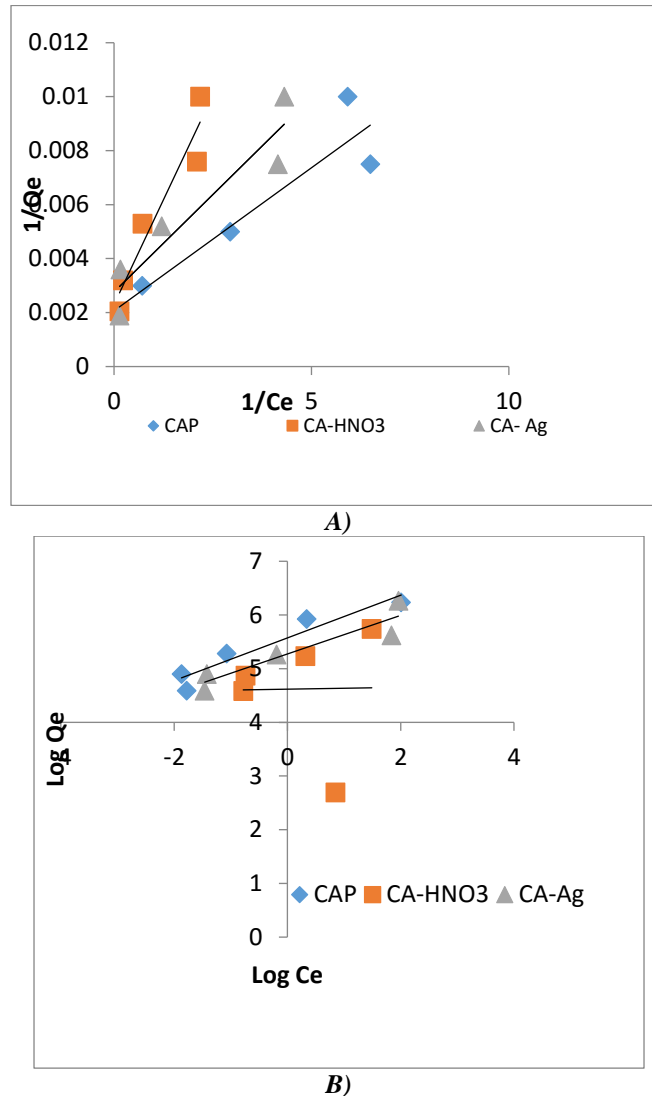


Fig. 5: The linear plots, (A) from Langmuir adsorption model and (B) from Freundlich adsorption model.

It was observed that the Freundlich isotherm better described the atrazine adsorption for PAC with the higher correlation coefficient  $R^2$  (0.913), suggesting that some heterogeneity on the surfaces or pores of PAC played an important role in atrazine adsorption and different sites with several adsorption energies were involved [10]. This agrees with the others works, where the Freundlich isotherm was more suitable than the Langmuir isotherm for the adsorption of atrazine on various adsorbents such as humics acids- silica gel mixtures [22], sewage sludge amended luvisolsol soil [23], multiwalled carbon nanotube [5]. However the atrazine adsorption was better fitted with the Langmuir Isotherm for -ACHNO<sub>3</sub> (Table 3), from which, it could be assumed that the adsorbed atrazine formed monolayer coverage on the adsorbent surface and all adsorption sites were equal with uniform adsorption energies without any interaction between the adsorbed molecules [21]. For AC-Ag, the isothermal data fitted well in Langmuir model and Freundlich model. The values of  $1/n < 1$  represent an advantageous adsorption conditions. Therefore, the Freundlich exponent  $1/n$  gave an indication of the favorable atrazine adsorption by all adsorbents which was also justified by the values of  $R_L < 1$ . The values of  $Q_m$  in Table 3 showed that the PAC samples have the highest affinity for atrazine removal than the AC-HNO<sub>3</sub> and AC-Ag. The adsorption performance of the samples for atrazine seems to follow the sequence PAC > AC-HNO<sub>3</sub> > AC-Ag. It is due to the increase of acidic groups on the surface of adsorbent

during the modification (Table 1). This suggested that the adsorption capacities decreased as the oxygen contents on the surface of adsorbent increased [6].

**Table 3: Parameters values of the isotherms for atrazine adsorption onto the PAC, AC-HNO<sub>3</sub> and AC-Ag.**

Isotherms	Paramètres	PAC	AC-HNO <sub>3</sub>	AC-Ag
Langmuir	R <sup>2</sup>	0.8849	0.918	0.8876
	Q <sub>m</sub> (mg/g)	476.19	434.78	357.14
	K <sub>L</sub> (L/mg)	1.9	0.74	2
	R <sub>L</sub>	0.02564	0.063	0.02439
Freundlich	R <sup>2</sup>	0.913	0.0001	0,8662
	K <sub>F</sub> (mg/g)	263.09	101.3013	195.09
	1/n	0.3977	0.0171	0.3595

## CONCLUSION

The batch technique was used to study the atrazine adsorption on three adsorbents: PAC, AC-HNO<sub>3</sub> and AC-Ag. The experimental data fitted well the pseudo-second order kinetic model. The equilibrium data followed the Freundlich isotherm for the PAC, the Langmuir isotherm for the AC-HNO<sub>3</sub> and the both isotherm models for the AC-Ag. However, these results revealed that the adsorption affinity decreased when the oxygen content on the surface increased. This study demonstrated that the surface functionalities have an influence on the removal performances of the three adsorbents used. Finally, as described by Langmuir, the maximum adsorption capacities obtained demonstrated that these adsorbents are potential materials for wastewater treatment.

## ACKNOWLEDGEMENT

The authors thank the Applied Organic Chemistry Laboratory of the Chemistry Department, Faculty of Science Semlalia, Cadi Ayyad University of Morocco, for the materials and logistics support.

## REFERENCES

- [1] Urena-AMate M. D, Socias-Viciano M, Gonzalez-Pradas E, and Saifi M, "Effect of ionic strength and temperature on adsorption of atrazine by heat treated kerolite" in *Chemosphere*, Vol. 59, Sept. 2005, pp. 69-74.
- [2] Zhang W, Zheng J, Pingping Z, and Qiu R, "Atrazine immobilization on sludge derived biochar and the interactive influence of coexisting pb(II) or Cr(VI) ions", in *Chemosphere*, Vol. 134, May. 2015, pp. 438-445.
- [3] Castro C. S, Guerreiro M. C, Goncalves M, Oliveira, L. C. A, and Anastacio A. S, "Activated carbon/ iron oxide composites for the removal of atrazine from aqueous medium", in *J. Hazard. Mater*, Vol. 164, August. 2009, pp. 609-614.
- [4] Seung-Woo N, Dae-Jin C, Seung-Kyu K, Her N, and Kyung-Duk Z, "Adsorption characteristics of selected hydrophilic and hydrophobic micropollutants in water using activated carbon", in *J. Hazard. Mater*, Vol. 270, Jan. 2014, pp. 144-152.
- [5] Wang-Wang T, Guang-ming Z, Ji-lai G, Yang L, Xi-yang W, Yuan- yuang L, Zhi-Feng L, Chen L, Xiu-Rong Z, and De-zhu T, "Simultaneous adsorption of atrazine and Cu(II) from wastewater by magnetic multi-walled carbon nanotube" in *Chem. Eng. J*, Vol. 211-212, Oct. 2012, pp. 470-478.
- [6] Guang-Cai C, Xiao-Quan S, Yi-Quan Z, Xiu-e S, Hong-lin H, and Shahamat U. K, "Adsorption, kinetics isotherms and thermodynamics of atrazine on surface oxidized multiwalled carbon nanotubes", in *J. Hazard. Mater*, Vol. 169, April. 2009, pp. 912-918.
- [7] Chingombe P, Saha B, and Wakema R. J, "Sorption of atrazine on conventional and surface modified activated carbon", in *J. colloid interface Sci*, Vol. 304, July. 2006, pp. 408-416.
- [8] Chunjing Z, Jinlong Y, Chunxiao Z, and Zhengpeng Y, "Enhanced adsorption of atrazine from aqueous solution by molecularly imprinted TiO<sub>2</sub> film", in *Solid state sci*, Vol. 14, April. 2012, pp.777-781.
- [9] Morales-pérez A. M, Arias C, and Ramirez-Zamora R, "Removal of atrazine from water using an iron photo catalyst supported on activated carbon", in *Adsorption*, DOI 10.1007/s10450-015-9739-8.

- [10] Jordi L, Conxita L, Ruiz B, Fuente E, Montserrat S, and Antonio D. D, "Role of activated carbon properties in atrazine and paracetamol adsorption equilibrium and kinetics", in *Process Saf. Environ. Prot.*, Vol. 95, Feb. 2015, pp. 51-59.
- [11] Amin Y. B, Rong W, and Rong X, "The effect of re-generable silver nanoparticle/ multi-walled Carbon nanotubes coating on the antibacterial performance of hollow fiber membrane", in *Chem. Eng. J.*, Vol. 230, June. 2013, pp. 251-259.
- [12] Karima E, Bacaoui A, Sergent M, and Yaacoubi A, "Application of fractional factorial and Doehlert designs for optimizing the preparation of activated carbons from Argan shells", *Chemom. Intell. Lab. Syst.*, Vol. 139, Sept. 2014, pp. 48-57.
- [13] Jianghua Q, Guanghui W, Yuncheng B, Danlin Z, and Yang C, "Effect of oxidative modification of coal tar pitch-based mesoporous activated carbon on the adsorption of benzothiophene and dibenzothiophene", in *Fuel Process Technol.*, Vol. 129, Sept. 2015, pp. 85-90.
- [14] Qingchung C, and Qingsheng W, "Preparation of carbon microspheres decorated with silver nanoparticles and their ability to remove dyes from aqueous solution", in *J. Hazard. Mater.*, Vol. 283, Sept. 2015, pp. 193-201.
- [15] Song X. H, Gunawan P, Jiang R. R, Leong S.S.J, and Wang K, Xu R, "Surface activated carbon nanospheres for fast adsorption of silver ions from aqueous solutions", in *J. Hazard. Mater.*, Vol. 194, May. 2011, pp. 162-168.
- [16] Yavuz G, and Zeki A, "Nitric acid modification of activated carbon produced from waste tea and adsorption of methylene blue and phenol", in *Appl. Surf. Sci.*, Vol. 313, June. 2014, pp. 352-359.
- [17] Tran Quoc T, Nguyen V.S, Hoang Thi K. D, Nguyen Hoang L, Beu Thu T, Nguyen Thi V. A, Nguyen Dinh H, and Nguyen Hoang H, "Preparation and properties of silver nanoparticles loaded in activated carbon for biological and environmental application" in *J. Hazard. Mater.*, Vol. 192, June. 2011, pp.1321-1329.
- [18] Ozcan A, and Ozcan A. S, "Adsorption of acid red 57 from aqueous solutions onto surfactant- modified sepiolite", in *J. Hazard. Mater.*, Vol. 125, Sept. 2005, pp. 252-259.
- [19] Kannan K, and Sundaram M. M, "kinetics and mechanism of removal of methylene blue by adsorption on various carbons-a comparative study", in *Dyes Pigments*, Vol. 51, May. 2001, pp. 25-40.
- [20] Khodaie M, Nahid G, Babak M, and Mohsen R, "Removal of methylene blue from wastewater by adsorption onto ZnCl<sub>2</sub> activated corn husk carbon equilibrium studies" in *J. chem.*, Vol. 2013, March. 2013, pp. 6.
- [21] Ndi N. J, and Ketcha, M. J, "The adsorption efficiency of chemically prepared activated carbon from cola nut shells by ZnCl<sub>2</sub> on methylene blue", in *J. chem.*, Vol. 2013, May. 2013, pp. 7.
- [22] Kovaivos L. D, Paraskeva C. A, and Koutsoukos P. G, "Adsorption of atrazine from aqueous solution on humic acid and silica", in *J. Colloid Interface Sci.*, Vol. 356, Sept. 2011, pp. 277-285.
- [23] Lima D. L. D, Silva C. P, Schneider R. J, and Esteves V. I, "Development of an Elisa procedure to study sorption of atrazine onto sewage sludge -amended luvisol soil", in *Talanta*, Vol. 85, Sept.2011, pp.1494-1499.